The neuroanatomical phenotype of tuberous sclerosis complex: focus on radial migration lines

Agnies M. van Eeghen · Laura Ortiz Terán ·
Jason Johnson · Margaret B. Pulsifer ·
Elizabeth A. Thiele · Paul Caruso

Abstract

Introduction The contribution of radial migration lines (RMLs) to the neuroanatomical and neurocognitive phenotype of tuberous sclerosis complex (TSC) is unclear. The aim of this study was to perform a comprehensive evaluation of the neuroradiological phenotype of TSC, distinguishing RMLs from normal-appearing white matter (NAWM) using diffusion tensor imaging (DTI) and volumetric fluid-attenuated inversion recovery imaging.

Methods Magnetic resonance images of 30 patients with TSC were evaluated. The frequencies of RMLs, tubers, and subependymal nodules (SENs) were determined for every hemispheric lobe. Cerebellar lesions and subependymal giant cell tumors were counted. DTI metrics were obtained from the NAWM of every hemispheric lobe and from the largest RML and tuber. Analyses of variance and correlations were performed to investigate the associations between neuroanatomical characteristics and relationships between RML frequency and neurocognitive outcomes. NAWM DTI metrics were compared with measurements of 16 control patients.

Results A mean of 47 RMLs, 27 tubers, and 10 SENs were found per patient, and the frequencies of these lesions were strongly correlated ($p < 0.001$). RML fractional anisotropy and mean diffusivity were strongly inversely correlated ($p = 0.003$). NAWM DTI metrics were similar to the controls ($p = 0.26$). RML frequency was strongly associated with age of seizure onset ($p = 0.003$), intelligence outcomes ($p = 0.01$), and level of autistic features ($p = 0.007$).

Conclusion A detailed neuroradiological phenotype is presented, showing that RMLs are the most frequent neuroanatomical lesion, are responsible for white matter DTI abnormalities, and are strongly associated with age of seizure onset, intelligence outcomes, and level of autistic features.

A. M. van Eeghen (✉) · E. A. Thiele
Department of Neurology, Carol and James Herscot Center
for Tuberous Sclerosis Complex, Massachusetts General Hospital,
175 Cambridge Street,
Boston, MA 02114, USA
e-mail: avaneeghen@partners.org

A. M. van Eeghen
ENCORE, Expertise Centre for Neurodevelopmental Disorders,
Department of Neuroscience, Erasmus Medical Centre,
Rotterdam, The Netherlands

L. O. Terán · J. Johnson · P. Caruso
Department of Radiology, Massachusetts General Hospital,
Boston, MA, USA

M. B. Pulsifer
Department of Psychiatry, Psychological Assessment Center,
Massachusetts General Hospital, Boston, MA, USA

Introduction

Tuberous sclerosis complex (TSC) is an autosomal dominant disorder caused by mutations in the tumor suppressor genes *TSC1* or *TSC2*. Loss of function of the TSC1–TSC2 protein complex causes upregulation of the mammalian target of rapamycin (mTOR) pathway, resulting in a tumor growth phenotype. Brain manifestations of TSC are variable in severity are characterized by cortical tubers, white matter (WM) abnormalities, and periventricular subependymal nodules (SENs) which may evolve into subependymal giant cell tumors (SGCTs) [1–3]. Neurocognitive morbidity is often severe, including early onset seizures (90 %), cognitive impairment (50 %), and psychiatric disorders (70 %) [4, 5]. Early diagnosis and interventions may improve

neurocognitive prognosis, inspiring an active search for neuroradiological prognostic biomarkers.

Historically, neuroimaging studies in TSC have focused on morphological tuber characteristics and their relationships with neurocognitive morbidity, reporting variable and conflicting results [6, 7]. With emerging evidence for WM dysconnectivity in TSC [8], imaging investigations shifted to WM microstructure using diffusion tensor imaging (DTI), which is sensitive to the molecular movement of water and provides information on WM integrity or pathology.

It was established that radial migration lines (RMLs) were associated with abnormal DTI values [9–14] (Fig. 1), consistent with the histopathological findings of disrupted myelination in these areas [15, 16]. Although these observations suggest that RMLs may contribute to neurocognitive morbidity in TSC, these lesions have only rarely been acknowledged as prognostic biomarkers [17, 18] and no quantitative evaluations have been performed.

Instead, recent studies have focused on DTI investigations in normal-appearing white matter (NAWM) with conflicting observations, reporting both normal [10, 13, 14] and abnormal NAWM microstructure [9, 19–22]. However, most investigations were limited by small sample sizes, low-resolution fluid-attenuated inversion recovery (FLAIR) imaging, or did not exclude regions with RMLs from their measurements. Findings that presumed that NAWM abnormalities were often regional [9, 11, 20–24] and correlated with the volume of "subcortical tubers" [23] suggest that the presence of RMLs interfered with these DTI measurements.

We hypothesized that, in TSC, the contribution of RMLs to the neuroradiological phenotype is underrecognized, that RMLs are responsible for microstructural WM abnormalities,

and that RMLs contribute to the neurocognitive phenotype of TSC. To explore the first hypothesis, a detailed morphological evaluation was performed, quantifying the distribution and frequencies of RMLs, tubers, SENs, and SGCTs. Secondly, RMLs and NAWM were interrogated with DTI under guidance of volumetric FLAIR imaging in TSC patients and control patients. Lastly, RML characteristics were compared with quantitative data on seizures, intelligence and autistic features.

Methods

Subjects

All subjects were followed at the multidisciplinary TSC clinic of the study institution and had a definite diagnosis of TSC [1]. The inclusion criteria were (1) the availability of a recent magnetic resonance imaging (MRI) study that met the study protocol criteria (see succeeding sections), free of motion or technical artifacts, obtained since 2009 and (2) at least 4 years of age, as after this myelin remodeling is limited. Exclusion criteria were neurosurgery within the last year. This study was approved by the institutional review board of the hospital.

Clinical information

Medical records were reviewed and the following information was recorded: date of birth, gender, history of seizures, history of infantile spasms (IS), age of onset of seizures, and history of neurosurgery. When available, full-scale intelligence quotients or developmental quotients (IQ/DQs) were retrieved.
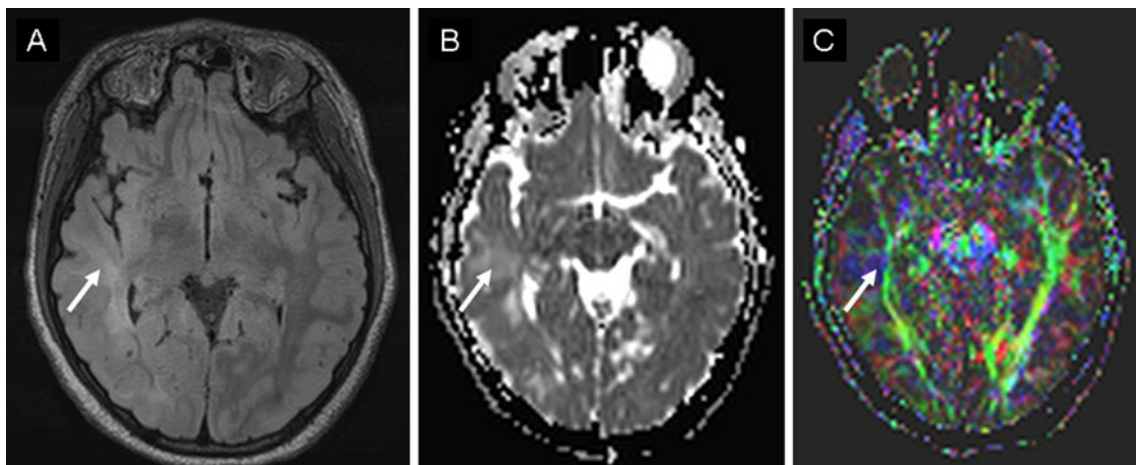

Fig. 1 Appearance of RMLs in a patient with TSC. **a** Axial volumetric FLAIR showing RML extending from the temporal horn of the right lateral ventricle to the right superior temporal gyrus (*arrow*). **b** ADC map showing increased MD in the area of the RML, suggesting disruption of the WM microstructure (*arrow*). **c** FA color map showing aberrant orientation of WM fibers in the area corresponding with the RML (*arrow*)

Behavioral measures

In the context of a larger study on TSC and neurobehavioral morbidity, psychometric questionnaires were prospectively distributed between 1 October 2010 and 1 April 2012. For this study, we retrieved scores of the *Social Communication Questionnaire* (SCQ), when available. The SCQ [25] is a reliable, validated screening instrument for ages 4 years and older. It yields a level of autistic features, based on current diagnostic criteria for the Autism Diagnostic Interview—Revised [26]. The scale is completed by a caregiver, and since it can also be used for nonverbal probands, it is suitable for all TSC patients [27]. For this study, the *T* scores of the SCQ-Lifetime were used.

Image acquisition

All MRIs were performed without gadolinium on a 3.0-T system (TimTrio; Siemens, Erlangen, Germany) as part of the diagnosis or annual routine follow-up. The imaging protocol included 3D volumetric T1-weighted sequence (flip angle, 7°; TR, 2,530 ms; TE, 1.64 ms; inversion time, 1,100 ms; voxel size, $1.0\times1.0\times1.0$ mm; section thickness (ST), 1.0 mm; acquisition matrix, 256×256; field of view (FOV), 26 cm; sagittal); T2-weighted turbo spin echo (TR, 6,380 ms; TE, 97 ms; voxel size, $0.4\times0.4\times4.0$ mm; ST, 4.0 mm; matrix, 442×512; FOV, 17–22 cm; 0 gap; axial), 3D turbo spin echo FLAIR (TR, 5,000 ms; TE, 355 ms; time to inversion, 1,800 ms; voxel size, $0.5\times0.5\times1.0$ mm; ST, 1 mm; matrix, 388×384; FOV, 19×19 cm; sagittal), and susceptibility-weighted imaging (SWI) (TR, 26 ms; TE, 19 ms; voxel size, $0.9\times1.0\times1.5$ mm; ST, 1.5 mm; matrix, 182×256; FOV, 17×23 cm). Diffusion tensor images were acquired in an axial plane and contained the following parameters: TR, 8,440 ms; TE, 90 ms; voxel size, $2.0\times2.0\times2.0$ mm; ST, 2 mm; imaging matrix, 128×128; FOV, 26×26 cm; 0 gap; diffusion directions, 25; *b* value, 1,000 s/mm^2. Images were eddy current corrected and processed to create fractional anisotropy (FA) and mean diffusivity (MD) maps.

Morphologic MRI evaluation

MRIs were evaluated by one of two radiologists: a pediatric neuroradiologist with 11 years post-fellowship experience (PC) and a radiologist specifically trained for the evaluation of TSC patients (LOT). Evaluations were performed after a review of five test cases where methods and lesion classification were established by consensus (AvE, LOT, and PC).

For the identification and counting of RMLs and tubers, the volumetric FLAIR images served as the primary data set, were reformatted on an AGFA PACs workstation, and viewed simultaneously in the axial, coronal, and sagittal planes. The axial T2, magnetization-prepared rapid gradient echo, and SWI sequences were consulted for clarification and to distinguish calcifications, cysts, and SENs.

Tubers were defined as cortically located lesions hyperintense to the normal cortex on the T2/FLAIR images that produced thickening or blurring of the normal cortex. RMLs were defined as curvilinear or band-shaped lesions traversing the deep WM and hyperintense to the NAWM on FLAIR or T2-weighted images (Fig. 1a). Tubers and RMLs were further evaluated for associated disruption of the gyral folding pattern and cystic and calcified components, and a nomenclature for morphological configurations was adopted (Online Resource 1).

SENs were defined as lesions originating from the ventricle wall and protruding into the ventricular lumen. SGCTs were defined as SENs that measured >1 cm; although this definition is clinically insufficient, it served our quantitative purpose. For patients with a history of SGCT resection, this SGCT was also counted. Cerebellar TSC lesions were defined as high-signal findings on the T2-weighted images. The hemispheric and lobar distributions of RMLs, tubers, and SENs were calculated.

Quantitative MRI analysis

Elliptical regions of interest (ROIs) were manually placed by an experienced radiologist (JJ) in consensus with a TSC research fellow with 2 years of experience with TSC neuroanatomy (AvE) after establishing a substantial interrater correlation with a pediatric neuroradiologist (PC) (see the "Statistical analysis" section). Using volumetric FLAIR images as anatomical reference, maximally sized ROIs (range, 20–100 mm^2) were placed on apparent diffusion coefficient (ADC) maps on (1) the largest RML and its contralateral WM region, (2) the largest tuber, and (3) the NAWM of every cerebral lobe in both hemispheres (OsiriX Dicom Viewer, Geneva). Because the frontal lobe is disproportionally large, two ROIs were placed per frontal hemispheric lobe: in the prefrontal WM and the more posterior WM (Online Resource 2). All ROIs were transposed on identical sections on the FA maps.

After excluding lobes where no NAWM could be visually detected, the mean MD and FA values of each lobe were averaged for each patient to approach a whole-brain index of NAWM MD and FA indices of the cerebral lobes. Cases where the largest RML or tuber were too small to allow a margin of at least 2 mm around the ROIs were excluded from the analysis of DTI metrics due to possible partial volume effects. Cystic or mineralized lesions were avoided as these have aberrant values. Lobes affected by neurosurgery were excluded from all analyses.

The MD and FA measurements of the same ROIs were obtained for 16 healthy control patients, including 7 children

(mean age, 9 years; range, 4–15 years) and 9 adults (mean age, 36 years; range, 29–41 years). Control images were retrospectively retrieved, and inclusion criteria included a normal MRI study using the same imaging protocol and the absence of neurological deficits or developmental delay.

Statistical analysis

To determine interrater agreement for the assessment of RMLs, tubers, and MD and FA values of tubers, RMLs, and NAWM, intraclass correlation coefficients (ICCs) were determined for a subset of 10 MRIs. An ICC of 0–0.20 indicated poor agreement; an ICC of 0.21–0.40, fair agreement; an ICC of 0.41–0.60, moderate agreement; an ICC of 0.61–0.80, substantial agreement; and an ICC of 0.81–1.00, nearly perfect agreement [28].

Analyses of variance (ANOVAs) and correlations were performed to (1) explore relationships between frequencies of RMLs, tubers, SENs, SGCTs, and cerebellar lesions, (2) test the association between the MD and FA of the largest RML and these macrostructural lesion frequencies, (3) compare RML frequency with intelligence outcomes, seizure variables, and age at MRI, and (4) compare NAWM DTI metrics of the cerebral lobes of TSC and control patients. Statistical analyses were performed using SPSS version 15.0 (SPSS Inc., Chicago, IL, USA). Confidence intervals were 95 %, and α was set at 0.05.

Results

Interrater agreement

For 10 MRIs, the ICCs between PC and LOT were $r=0.71$ for RMLs and $r=0.80$ for tubers, indicating substantial agreement. The remaining MRIs were reviewed by both PC (10) and LOT (10).

For DTI indices, the interrater correlation between PC and JJ/AvE was 0.93 for RML MDs, 0.80 for contralateral NAWM MD, and 0.74 for mean lobar NAWM MD values, indicating substantial to nearly perfect agreement. These agreements were the same for FA values. The MD/FA measurements by JJ/AvE were used for further analyses.

Patient characteristics

The MRIs of 30 patients (13 males and 17 females) were included, with a mean age at time of MRI of 15.5 years (range, 5–51 years). Of these patients, 23 (77 %) had a history of epilepsy, 8 (29 %) had a history of IS, and 11 (37 %) had refractory epilepsy. Eight patients had a history of neurosurgery: six received epilepsy surgery and two underwent SGCT resection. Twelve (40 %) of the patients had an intellectual disability (IQ<70). Of the 28 patients

who received genetic mutation analysis, 11 (39 %) showed a TSC1 mutation, 15 (54 %) had a TSC2 mutation, and in two (7 %) patients, no mutation was identified.

Morphological and microstructural relationships

The neuroradiological characteristics of the study group are listed in Table 1. All patients showed RMLs and 29 (97 %) patients showed tubers. Fifty-seven percent of RMLs extended into a tuber. Isolated tubers were rare (3 %), small, and not cystic or mineralized. RML frequency, tuber frequency, and SEN frequency were significantly correlated ($p \le 0.001$, $r > 0.56$ for all comparisons; Fig. 2a). RMLs, tubers, and SENs were equally distributed over the hemispheres. Compared with normal lobar proportional volumes [29], RMLs and tubers seemed to be slightly overrepresented in the frontal and occipital lobes (Online Resource 3). A trend was observed between the age at MRI and the frequency of RMLs ($p=0.06$).

After excluding five patients where partial volume effects may have influenced RML ROI measurements, a significant negative correlation was found between the MD and FA of the largest RML ($p=0.003$, $r=-0.56$). Interestingly, the MD of the largest RMLs were associated with higher frequencies of RMLs ($p=0.10$, $r=0.33$), tubers ($p=0.05$, $r=0.39$), and SENs ($p=0.006$, $r=0.55$), although only the latter comparisons were

Table 1 Neuroanatomical characteristics of the study group

	$N \pm$ SD (range)
Morphological characteristics	
RMLs	47±19 (4–86)
Tubers	27±16 (0–76)
Tuber–RML units	28±16(0–76)
Without gyral distortion	6±4 (0–23)
With gyral distortion	18±12 (0–40)
Cystic tubers	3±5 (0–19)
Mineralized	1±0.8 (0–6)
Isolated tubers	0.43±0.7 (0–5)
Isolated RMLs	20±15(2–48)
SENs	10±6 (0–22)
No. of patients with SEN >1 cm	13 (43 %)
No. of patients with cerebellar lesion	7 (23 %)
DTI characteristics (mean and standard deviation)	
MD tuber (×10^{-6} mm^2/s)	1,196±225 (909–1,863)
MD RML (×10^{-6} mm^2/s)	1,120±190 (826–1,576)
FA RML	0.23±0.06 (0.31–0.37)
MD NAWM (×10^{-6} mm^2/s)	758±60.0 (633–844)
FA NAWM	0.44±0.12 (0.31–0.53)

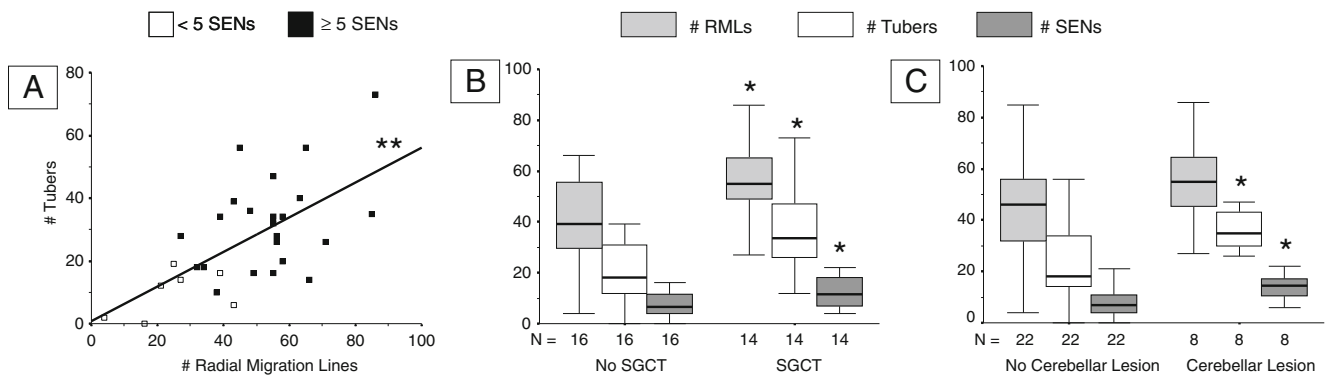*N* number, *SD* standard deviation, *NAWM* normal-appearing white matter

Fig. 2 Graphs depicting the associations between morphological neuroanatomical characteristics of the study group. **a** Scatter plot showing the correlation between the frequency of RMLs and tubers, showing categories of SEN frequencies. **b** Box plot depicting the association between the (history of) SGCT and frequencies of RMLs, tubers, and SENs. **c** Box plot depicting the association between cerebellar lesions and frequencies of RMLs, tubers, and SENs. *Box* 25th–75th percentile, *horizontal line* 50th percentile. *$p<0.01$; **$p<0.001$

significant. The largest RML FA showed no significant associations with lesion frequencies ($p>0.20$ for all comparisons).

There was a trend towards co-occurrence of SGCTs and cerebellar lesions ($p=0.06$). Patients with SGCTs showed significantly more RMLs ($p=0.01$), tubers ($p=0.005$), and SENs ($p=0.01$), but no significant differences in DTI metrics of RMLs or tubers ($p>0.10$ for all comparisons) (Fig. 2b). Patients with cerebellar lesions showed significantly more tubers ($p=0.007$) and SENs ($p=0.01$), but no significant differences in RML frequency ($p=0.17$) or differences in DTI values of RMLs and tubers ($p>0.4$ for all comparisons) (Fig. 2c).

Relationship between RMLs and the neurocognitive phenotype

Highly significant relationships were observed between frequency of RMLs and quantitative neurocognitive outcomes such as age of seizure onset, IQ/DQs, and rate of autistic features (Table 2). Associations with dichotomous variables such as a history of IS were weaker.

Table 2 Results of statistical analysis showing bivariate associations between RML frequency and neurodevelopmental outcomes, depicting p values for ANOVAs and correlations

	RML frequency
Age at MRI	0.06 ($r=-0.34$)
History of epilepsy	0.05
History of infantile spasms	0.12
Age of seizure onset	0.003 ($r=-0.60$)
IQ/DQ	0.01 ($r=0.48$)
Rate of autistic features[a]	0.007 ($r=0.56$)

Clinical data were available for all patients, IQ/DQ scores were available for 26 patients, and SCQ scores were available for 22 patients

ANOVA analysis of variance, *r* correlation coefficient, *IQ/DQ* intelligence/developmental quotient

[a] As measured by the SCQ (see the "Methods" section)

NAWM characteristics

Of all supratentorial hemispheric lobes, no NAWM could be detected in 105 (35 %) lobes of 25 patients. After exclusion of these lobes, TSC and control patients did not show significant differences for mean supratentorial lobar NAWM MD and FA values ($p=0.26$ for both comparisons) (Fig. 3). The DTI metrics of cerebellar NAWM were normal and similar for cerebellar lobes with our without a lesion ($p>0.48$ for all comparisons).

Discussion

Our findings suggest that RMLs are the most frequent neuroanatomical lesion in TSC patients and are strongly
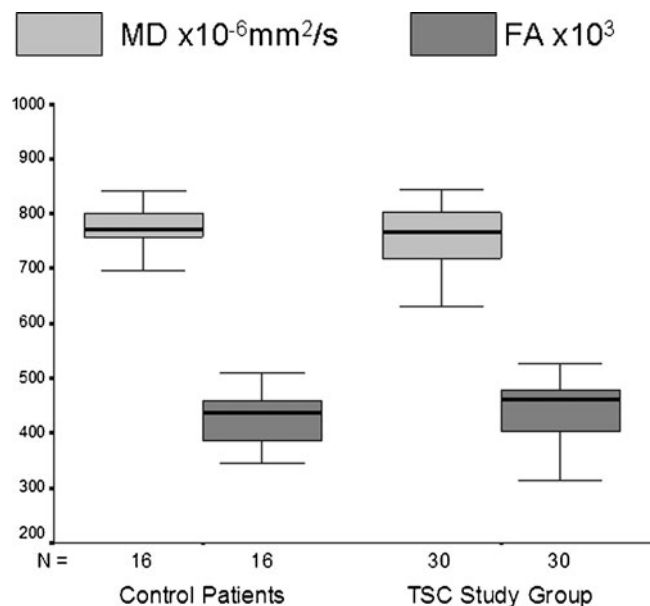

Fig. 3 Box plot comparing the DTI metrics of NAWM of TSC patients and control patients. No statistical difference was found between the two groups. *Box* 25th–75th percentile, *horizontal line* 50th percentile

associated with neurocognitive morbidity. The combination of DTI and high-resolution FLAIR imaging allowed these focal migration abnormalities to be distinguished from normal brain parenchyma, demonstrating that RMLs are responsible for DTI abnormalities in the cerebral lobes.

Characteristics of RMLs

The observed average frequency of 47 RMLs compellingly resembles the mean of 46 morphological abnormalities found in a recent neuropathological study [30]. Only about half of these RMLs terminated in a tuber, and RMLs without cortical involvement were generally smaller. In the RMLs, the MD, reflecting the magnitude of water diffusion regardless of the direction, and the FA, reflecting the degree of directionality of the diffusion, were abnormal and inversely correlated. This is similar to previous observations in TSC [13, 14, 31] and in WM associated with other malformations of cortical development [32]. The observation that the NAWM DTI metrics of the cerebral lobes of TSC patients were similar to that of control patients underlines that WM abnormalities in TSC are not diffuse and reflect focal migration abnormalities rather than other causes of disconnectivity. In this regard, we prefer "radial migration line" to previous nomenclature such as "subcortical tubers," hamartomas, or radial glial bands. Although the observed trend towards more RMLs at a younger age is probably due to referral bias, future research should investigate features of RMLs in utero and in early childhood.

Contribution of RMLs to the neuroradiological phenotype

The strong correlations between the frequencies of RMLs, tubers, and SENs confirm that these lesions originate from a common biological dysfunction in the periventricular zone. Since these lesions show also histological similarities [15, 16, 33] and evidence of mTOR dysregulation [34], RMLs, SENs, and tubers should be regarded as an inextricable triad representing aberrant proliferation and migration in TSC. Solely identifying patients by tubers or SENs may lead to a misleading conclusion of a "negative" MRI at a time where intervention may greatly improve neurodevelopmental prognosis. Hence, we advocate combining tubers and RMLs into one major diagnostic criterion.

The significant associations between the MD of the largest RML and lesion frequencies support histological observations that both lesion frequency and severity may covary with mTOR dysregulation [30]. Furthermore, patients with SGCTs and cerebellar lesions showed more RMLs, tubers, and SENs, suggesting that lesion frequency may help stratify patients at risk for SGCT growth. However, due to partial volume effects, only the largest RMLs could be interrogated with DTI metrics, limiting our analyses between lesion frequency, severity, and growth.

The exact mechanisms by which enhanced mTOR signaling leads to migration deficits are unclear. mTOR is expressed during early brain development in progenitor cells in the ventricular zone and in early neuronal cells in the nascent cortical plate. Loss of function of regulatory genes that are expressed simultaneously with mTOR, such as *TSC1* and *TSC2*, *PTEN*, and *NF1* [35, 36], would result in dysregulated mTOR activity, causing disturbed proliferation of neural and astrocytic precursor cells and cytomegaly, compromising neuronal migration and differentiation.

Relationship between RMLs and the neurocognitive phenotype

The frequency of RMLs was strongly associated with the age of seizure onset and a history of seizures, underlining that WM migration deficits are a robust biomarker for these important prognostic outcomes. Although this association could be explained by the strong relationship between RML and tuber frequency, and a subcortical origin of seizures is controversial, our observations add to evidence of epileptic discharges in regions without tubers [37] or outside of tubers [38]. Together with observations of seizures in a TSC mouse model with only subcortical lesions [39] and neurosurgical experience that relatively large resections of cortex and WM are often necessary to achieve seizure freedom [40], our findings suggest that WM should be included in investigations in epilepsy studies.

Compellingly, RML frequency was also strongly associated with the level of intelligence and rate of autistic features, concordant with observations that these variables are inextricably linked with age at seizure onset [41]. Together with our findings of normal NAWM microstructure, our results suggest that, in TSC, neurocognitive deficits are suggest that, in TSC, neurocognitive deficits are caused by focal migration and proliferation abnormalities, rather than primary, global synaptic dysfunction primary, global synaptic dysfunction. By interfering with the development of neural circuitry, RMLs could impair neurotransmission, resulting in seizures and deficits in intelligence, communication, and social skills. The regional distribution of RMLs may particularly affect longer-ranging WM tracts, concordant with a previous observation that impaired WM integrity of the corpus callosum was associated with autistic features [24].

Since quantifying RMLs was extremely laborious, the observed strong associations with neurocognitive outcomes and DTI and FLAIR abnormalities should encourage research on automated methods for evaluating whole-brain WM diffusivity or hyperintensity indices as potential biomarkers. DTI may well detect brain abnormalities before conventional MRIs in early childhood or even prenatally, which is particularly critical in the context of administration of neuroprotective therapies.

Limitations

Although our study population was relatively large, the number of our analyses exceeded that allowed for this sample size and should be regarded as exploratory. Distinguishing NAWM from multifocal dysplasia is complex in TSC; the variable distribution of RMLs does not allow standardized ROI placement or using a template, which may introduce data variability. However, we established acceptable interrater correlations and further increased the confidence level of our validity for the NAWM DTI metrics by including one ROI in every lobe, and even two ROIs in the frontal lobe, and taking the average of these measurements. This is the first study to exclude lobes without visible NAWM, making this the most detailed NAWM analysis in TSC. Since NAWM was detected in every patient and all indices contributed equally to the analyses, selection bias was limited.

Since most of the study patients had a positive history of epilepsy, observed DTI changes could be related to sequelae of chronic seizures, such as neuronal loss and gliosis. However, the normal DTI measurements in the NAWM of our patients suggest that aberrant FA and MD values in patients with TSC are relatively specific for the presence of RMLs. We did not address the FA of tubers to limit our comparisons as FA abnormalities in tubers have been well established and RMLs were the focus of this paper.

Conclusion

This study suggests that, in TSC, disruptions in cerebral neural circuitry are not diffuse, but primarily determined by focal migration abnormalities. RMLs are the most pervasive neuroanatomical feature, are the major contributor to WM microstructural abnormalities, and are strongly associated with neurocognitive morbidity. These observations pave the way for studies on whole-brain DTI parameters as a biomarker for neurocognitive morbidity in TSC.

References

1. Roach ES, Sparagana SP (2004) Diagnosis of tuberous sclerosis complex. J Child Neurol 19:643–649
2. Ridler K, Bullmore ET, De Vries PJ, Suckling J, Barker GJ, Meara SJ, Williams SC, Bolton PF (2001) Widespread anatomical abnormalities of grey and white matter structure in tuberous sclerosis. Psychol Med 31:1437–1446
3. DiMario FJ Jr (2004) Brain abnormalities in tuberous sclerosis complex. J Child Neurol 19:650–657
4. Muzykewicz DA, Newberry P, Danforth N, Halpern EF, Thiele EA (2007) Psychiatric comorbid conditions in a clinic population of 241 patients with tuberous sclerosis complex. Epilepsy Behav 11:506–513
5. Chu-Shore CJ, Major P, Camposano S, Muzykewicz D, Thiele EA (2010) The natural history of epilepsy in tuberous sclerosis complex. Epilepsia 51:1236–1241
6. Jansen FE, Vincken KL, Algra A, Anbeek P, Braams O, Nellist M, Zonnenberg BA, Jennekens-Schinkel A, van den Ouweland A, Halley D, van Huffelen AC, van Nieuwenhuizen O (2008) Cognitive impairment in tuberous sclerosis complex is a multifactorial condition. Neurology 70:916–923
7. Wong V, Khong PL (2006) Tuberous sclerosis complex: correlation of magnetic resonance imaging (MRI) findings with comorbidities. J Child Neurol 21:99–105
8. Nie D, Di Nardo A, Han JM, Baharanyi H, Kramvis I, Huynh T, Dabora S, Codeluppi S, Pandolfi PP, Pasquale EB, Sahin M (2010) Tsc2-Rheb signaling regulates EphA-mediated axon guidance. Nat Neurosci 13:163–172
9. Garaci FG, Floris R, Bozzao A, Manenti G, Simonetti A, Lupattelli T, Curatolo P, Simonetti G (2004) Increased brain apparent diffusion coefficient in tuberous sclerosis. Radiology 232:461–465
10. Karadag D, Mentzel HJ, Gullmar D, Rating T, Lobel U, Brandl U, Reichenbach JR, Kaiser WA (2005) Diffusion tensor imaging in children and adolescents with tuberous sclerosis. Pediatr Radiol 35:980–983
11. Peng SS, Lee WT, Wang YH, Huang KM (2004) Cerebral diffusion tensor images in children with tuberous sclerosis: a preliminary report. Pediatr Radiol 34:387–392
12. Piao C, Yu A, Li K, Wang Y, Qin W, Xue S (2009) Cerebral diffusion tensor imaging in tuberous sclerosis. Eur J Radiol 71:249–252
13. Firat AK, Karakas HM, Erdem G, Yakinci C, Bicak U (2006) Diffusion weighted MR findings of brain involvement in tuberous sclerosis. Diagn Interv Radiol 12:57–60
14. Sener RN (2002) Tuberous sclerosis: diffusion MRI findings in the brain. Eur Radiol 12:138–145
15. Boer K, Troost D, Jansen F, Nellist M, van den Ouweland AM, Geurts JJ, Spliet WG, Crino P, Aronica E (2008) Clinicopathological and immunohistochemical findings in an autopsy case of tuberous sclerosis complex. Neuropathology 28:577–590
16. Griffiths PD, Hoggard N (2009) Distribution and conspicuity of intracranial abnormalities on MR imaging in adults with tuberous sclerosis complex: a comparison of sequences including ultrafast T2-weighted images. Epilepsia 50:2605–2610
17. Shepherd CW, Houser OW, Gomez MR (1995) MR findings in tuberous sclerosis complex and correlation with seizure development and mental impairment. Am J Neuroradiol 16:149
18. Numis AL, Major P, Montenegro MA, Muzykewicz DA, Pulsifer MB, Thiele EA (2011) Identification of risk factors for autism spectrum disorders in tuberous sclerosis complex. Neurology 76:981–986
19. Widjaja E, Simao G, Mahmoodabadi SZ, Ochi A, Snead OC, Rutka J, Otsubo H (2010) Diffusion tensor imaging identifies changes in normal-appearing white matter within the epileptogenic zone in tuberous sclerosis complex. Epilepsy Res 89:246–253
20. Makki MI, Chugani DC, Janisse J, Chugani HT (2007) Characteristics of abnormal diffusivity in normal-appearing white matter investigated with diffusion tensor MR imaging in tuberous sclerosis complex. AJNR Am J Neuroradiol 28:1662–1667
21. Arulrajah S, Ertan G, Jordan L, Tekes A, Khaykin E, Izbudak I, Huisman TA (2009) Magnetic resonance imaging and diffusion-weighted imaging of normal-appearing white matter in children and young adults with tuberous sclerosis complex. Neuroradiology 51:781–786

22. Krishnan ML, Commowick O, Jeste SS, Weisenfeld N, Hans A, Gregas MC, Sahin M, Warfield SK (2010) Diffusion features of white matter in tuberous sclerosis with tractography. Pediatr Neurol 42:101–106

23. Simao G, Raybaud C, Chuang S, Go C, Snead OC, Widjaja E (2010) Diffusion tensor imaging of commissural and projection white matter in tuberous sclerosis complex and correlation with tuber load. AJNR Am J Neuroradiol 31:1273–1277

24. Peters JM, Sahin M, Vogel-Farley VK, Jeste SS, Nelson CA 3rd, Gregas MC, Prabhu SP, Scherrer B, Warfield SK (2012) Loss of white matter microstructural integrity is associated with adverse neurological outcome in tuberous sclerosis complex. Acad Radiol 19:17–25

25. Berument SK, Rutter M, Lord C, Pickles A, Bailey A (1999) Autism screening questionnaire: diagnostic validity. Br J Psychiatry 175:444–451

26. Lord C, Rutter M, Le Couteur A (1994) Autism Diagnostic Interview-Revised: a revised version of a diagnostic interview for caregivers of individuals with possible pervasive developmental disorders. J Autism Dev Disord 24:659–685

27. Granader YE, Bender HA, Zemon V, Rathi S, Nass R, Macallister WS (2010) The clinical utility of the Social Responsiveness Scale and Social Communication Questionnaire in tuberous sclerosis complex. Epilepsy Behav 18:262–266

28. Widjaja E, Zarei Mahmoodabadi S, Otsubo H, Snead OC, Holowka S, Bells S, Raybaud C (2009) Subcortical alterations in tissue microstructure adjacent to focal cortical dysplasia: detection at diffusion-tensor MR imaging by using magnetoencephalographic dipole cluster localization. Radiology 251:206–215

29. Allen JS, Damasio H, Grabowski TJ (2002) Normal neuroanatomical variation in the human brain: an MRI-volumetric study. Am J Phys Anthropol 118:341–358

30. Marcotte L, Aronica E, Baybis M, Crino PB (2012) Cytoarchitectural alterations are widespread in cerebral cortex in tuberous sclerosis complex. Acta Neuropathol (Berl) 123:685–693

31. Jansen FE, Braun KP, van Nieuwenhuizen O, Huiskamp G, Vincken KL, van Huffelen AC, van der Grond J (2003) Diffusion-weighted magnetic resonance imaging and identification of the epileptogenic tuber in patients with tuberous sclerosis. Arch Neurol 60:1580–1584

32. Widjaja E, Blaser S, Miller E, Kassner A, Shannon P, Chuang SH, Snead OC 3rd, Raybaud CR (2007) Evaluation of subcortical white matter and deep white matter tracts in malformations of cortical development. Epilepsia 48:1460–1469

33. Mizuguchi M, Takashima S (2001) Neuropathology of tuberous sclerosis. Brain Dev 23:508–515

34. Wong M, Crino PB (2012) Tuberous sclerosis and epilepsy: role of astrocytes. Glia 23:508–515

35. Crino PB (2011) mTOR: a pathogenic signaling pathway in developmental brain malformations. Trends Mol Med 17:734–742

36. da Lee Y, Yeh TH, Emnett RJ, White CR, Gutmann DH (2010) Neurofibromatosis-1 regulates neuroglial progenitor proliferation and glial differentiation in a brain region-specific manner. Genes Dev 24:2317–2329

37. Gallagher A, Chu-Shore CJ, Montenegro MA, Major P, Costello DJ, Lyczkowski DA, Muzykewicz D, Doherty C, Thiele EA (2009) Associations between electroencephalographic and magnetic resonance imaging findings in tuberous sclerosis complex. Epilepsy Res 87:197–202

38. Major P, Rakowski S, Simon MV, Cheng ML, Eskandar E, Baron J, Leeman BA, Frosch MP, Thiele EA (2009) Are cortical tubers epileptogenic? Evidence from electrocorticography. Epilepsia 50:147–154

39. Waltereit R, Welzl H, Dichgans J, Lipp HP, Schmidt WJ, Weller M (2006) Enhanced episodic-like memory and kindling epilepsy in a rat model of tuberous sclerosis. J Neurochem 96:407–413

40. Weiner HL, Carlson C, Ridgway EB, Zaroff CM, Miles D, LaJoie J, Devinsky O (2006) Epilepsy surgery in young children with tuberous sclerosis: results of a novel approach. Pediatrics 117:1494–1502

41. van Eeghen A, Pulsifer M, Merker V, Neumeyer A, van Eeghen E, Thibert R, Cole A, Leigh F, Plotkin S, Thiele E (2013) Understanding relationships between autism, intelligence, and epilepsy: a cross-disorder approach. Dev Med Child Neur 55:146–153